INITIATION OF FATIGUE CRACKS AT NON-METALLIC INCLUSIONS IN LARGE FORGINGS

C. Berger*, K. H. Mayer, W. Oberparleiter*** and R. B. Scarlin******

**KWU Mülheim, Federal Republic of Germany*
***MAN Nürnberg, Federal Republic of Germany*
****IABG Ottobrunn, Federal Republic Germany*
*****BBC Baden, Switzerland*

ABSTRACT

A method based on fracture mechanics is required for the prediction of the fatigue load level at which cracks can develop at specific inclusion areas present in large forgings.

The results of an investigation of four large forgings containing inclusions of different chemical compositions, morphology, distribution and size indicate that the evaluation of the fatigue cracking behaviour of steel-making inclusions can be performed satisfactorily using linear elastic fracture mechanics principles provided that the inclusions are present in the form of regions containing densely packed particles. On the other hand, the effect of single inclusions not consisting of densely packed regions may be overestimated.

KEYWORDS

Crack initiation; pulsation loading; low-cycle fatigue; rotor steels; interaction of flaws; fracture mechanic analyses;

INTRODUCTION

Even when using the most modern methods for the manufacture of large forgings it is still possible for individual non-metallic inclusions and groups of such defects to be trapped within the material.

A method based on fracture mechanics is required for the prediction of the fatigue load level at which cracks can develop at specific inclusions present. The method must be able to deal with inclusions of irregular shape and with groups of inclusions. It is conceivable that present practice in which such flaws are considered to act as sharp cracks and groups of defects are equated to a circle of size sufficient to enclose all defects in a group may be pessimistic. The period required to nucleate the crack and grow cracks in a group until they join up is neglected.

Previous results have shown that in the high cycle range the initiation of cracks both in a high strength 12 % Cr-steel (Friedl 1981) and in hardened and tempered low alloy steels (Harkegard, 1974) can be described using linear elastic fracture mechanics. Elsender et al (1977) performed pulsating tension low cycle fatigue tests up to 25,000 cycles on specimens containing alumino silicates in 3.5 % Ni and CrMoV steels, predominantly in the form of surface defects. They observed a good correlation with the threshold for fatigue crack propagation for individual defects and found no evidence for an incubation time before growth occurred if the stress intensity factor lay above the threshold value.

The aim of the present investigation was an extension of this work to different steel types showing a wide range in yield strength values and containing inclusions of different chemical composition, morphology, distribution and size both in the form of individual defects and groups of defects which would be expected to interact (clouds of irresolvable inclusions) in order to investigate methods for the quantitative evaluation of the effect of inclusions on fatigue properties. The present investigation was limited to the range up to 25,000 loading cycles to simulate the situation arising during start-up and shutdown of power generating equipment.

TESTING PROCEDURE

Four forgings were examined in the present work. Details of the manufacturing procedure, component type, size, chemical analyses and mechanical properties of adjacent, defect-free material are shown in Table 1. The forgings are designated A, D, G, and H and comprise a 1 % CrNiMo steel shaft of low yield strength (360 MPa), a 3.5 % Ni steel disc of high yield strength (880 MPA), a 2 % Cr 1 % Ni steel disc and a creep resistant 1 % CrMoV shaft.

Table 1: Description of Forgings and their Chemical Composition and Mechanical Properties

	Material	Forging	Dimensions	Melting procedure 1)	Ingot weight MPa	$R_{p0.2}$ MPa	Impact energy 20° J	$FATT_{50}$ °C	C	Si	Mn	P	S	Al	Cr	Mo	Ni	V
A	26CrNiMo 4	Shaft	Ø965,Ø615x8340	El and Vac	38	366	29-77	+30	.21	.24	.74	.006	.006	.004	1.10	.26	0.52	.01
D	28NiCrMoV145	Disc	$Ø_0$2520,$Ø_I$730 x530	El	100	884	61	-30	.28	.12	.22	.008	.011	.015	1.61	.43	3.50	.10
G	23CrNiMo747	Disc	$Ø_0$1720x620	El and CAP	12	660	98	+ 5	.23	.09	.74	.014	.009	.003	1.80	.72	1.07	.05
H	21CrMoV 511	Shaft	Ø1150,Ø300 x1100	El	--	640	62-70	+50	.23	.31	.37	.010	.009	.007	1.29	.97	0.24	.26

1) El- electric arc . Vac - vacuum degassed, CAP - Calcium Argon Procedure

Table 2 provides a summary of the results of the ultrasonic tests (equivalent disc reflector ER) along with the findings of the microstructural investigations. The findings may be summarized as follows:

A: Separate and grouped elliptical defects of ≦ 5 mm ER (Al_2O_3)
D: Separate circular defects of ≦ 4 mm ER (Al_2O_3/MnS)
G: Grouped irregular defects of ≦ 1 mm ER (silicates)
H: Separate and grouped irregular defects of ≦ 3 mm ER (MnS)

TABLE 2: Microstructure and Defect Type

Forging	Defect category ER 1)	Microstructure	Grain size ASTM	Defect type	Geometrical form 3)
Shaft A	I and C 2) ≤5 mm	Bainite and Ferrite and Pearlite	4 - 5	Predominantly Al_2O_3 densily packed particles, separated by areas of weak bounderies	elliptical
Disc D	I ≤4 mm	Bainite and Martensite	7 - 8	Al_2O_3/ MnS, non-uniformly distributed	irregular circular
Disc G	C ≤1 mm	Bainite and Martensite	3 - 4	small densily packed Calcium-Aluminium-Silicate particles	irregular equiaxed or elongated
Shaft H	I and C ≤3 mm	Ferrite and Pearlite	7 - 8	MnS particles (type II and III) also associated with pores	dendritic and compact irregular, approx. equiaxed

1) ER - Equivalent disc reflector 2) I - individual defect C - defect cluster 3) see typical photographs in Fig. 2

Round specimens of 30 mm diameter were machined from the defective regions of the forgings in such a direction that the loading was predominantly normal to the plane in which the defects lay. The specimens were then subjected to pulsating tension loading (R of 0.1) for up to 25,000 cycles at room temperature or until potential drop measurements indicated that significant crack growth had occurred. The experimental setup is shown in Fig. 1.

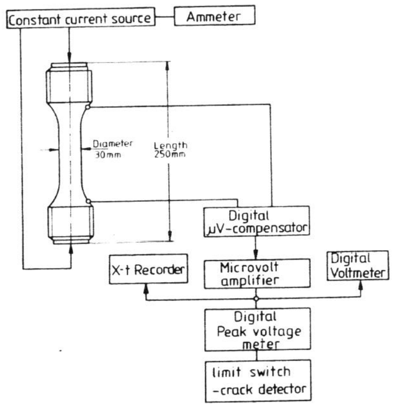

Fig. 1

Experimental testing arrangement

Various stress amplitudes were used providing maximum stress values between 66 % and 98 % of the yield strength level. After termination of the fatigue loading experiments the specimens were cooled in liquid nitrogen and broken open in a brittle manner. The fracture surfaces were examined in the optical and scanning electron microscope for evidence of the inclusions and nucleated fatigue cracks. Particular attention was paid to evidence of interaction between defects. At higher magnification the fatigue crack regions could be clearly identified and distinguished from the surrounding brittle overload failure. Figure 2 shows the appearance of typical fracture surfaces for each forging. Chemical composition of the inclusions was confirmed using an X-ray diffractometer in the scanning microscope. For all forgings it was possible to observe flaws at which fatigue cracks had nucleated and

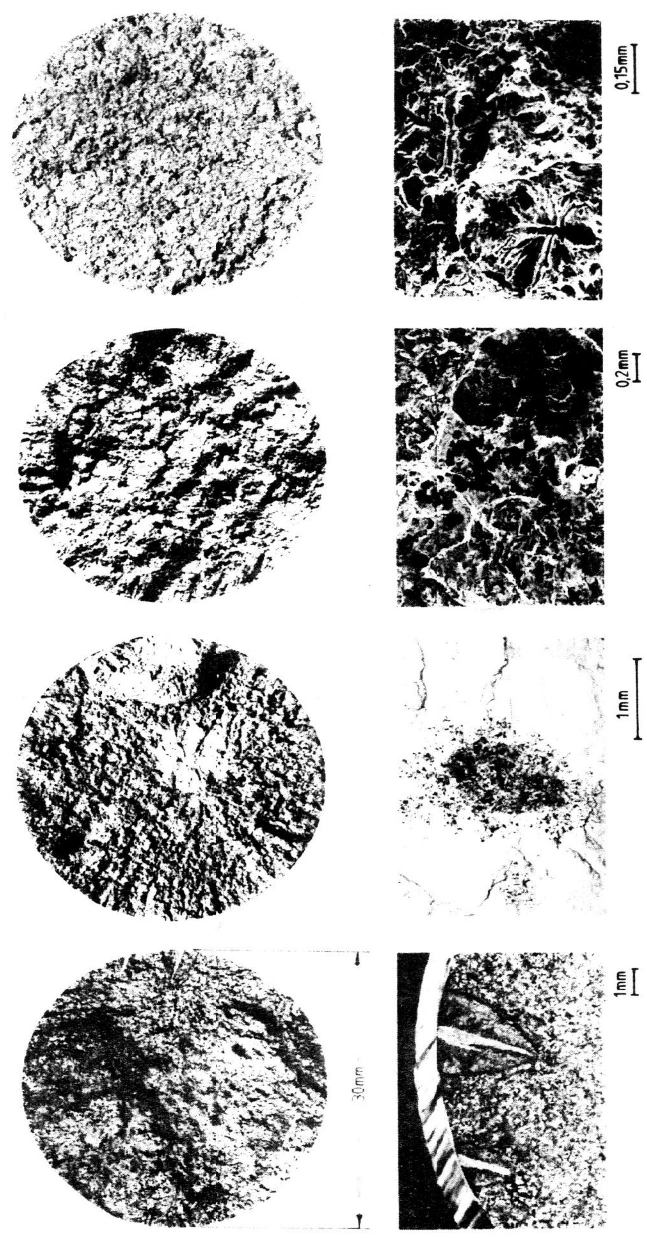

a: FORGING A
Elliptical inclusion area densely packed with Al_2O_3 particles (intermediate areas with weak bonding)
max. flaw area: 7,5 mm^2

b: FORGING D
Irregular inclusion area with non-uniformly distributed Al_2O_3/MnS
max. flaw area: 4,5 mm^2

c: FORGING G
Irregular equiaxed or elongated inclusion area densely packed with silicate particles
max. flaw area: 1 mm^2

d: FORGING H
Irregular approx. equiaxed inclusion area densely packed with MnS particles (also associated with pores)
max. flaw area: 0,3 mm^2

Fig. 2: Typical flaw appearances

others present in the brittle overload region but at which no crack had nucleated during fatigue loading. Observation of the fracture surfaces showed that although the US inspection of forging "A" showed grouped and separate flaws for all 28 flaws seen on the fracture surfaces the separations between their edges was greater than their individual widths. Since Melville (1976) has shown that the stress fields of neighbouring cracks will only interact at smaller separations these will be considered to be separate defects from the point of view of the fracture mechanics analysis. In a similar way the separations between flaws on the fracture surfaces of forging "G" specimens were large enough to preclude fracture mechanics interactions even though the US inspection indicated group defects (see Table 2).

On the other hand some of the flaws which appeared as separate US indications in specimens from forgings "D" and "H" in fact comprise closely spaced groups of inclusion areas which are sufficiently close together for interaction to occur. In these cases the flaws in such a group were evaluated together.

For the fracture mechanics evaluation a stress intensity value was assigned to each flaw (or group) observed on the fracture surface in the following way:

- For forging "A" in which compact inclusions with elliptical form are present separated by areas of weak bonding the elliptical form was adopted and the major and minor axes measured. The stress intensity amplitude is given by

$$\Delta K = \Delta\sigma \sqrt{\frac{\pi a}{Q}} \quad \ldots\ldots\ldots\ldots \quad (1)$$

where $\Delta\sigma$ is the stress amplitude, a the semi-minor axis of the ellipse, Q is the appropriate shape factor for the observed elliptical form. For inclusions which intersect the specimen surface the value of ΔK is increased by a factor of 1.12.

In the case of individual areas with densely packed particles (forging "G") the flaw shapes were intentionally approximated to a circle of the same area as the observed inclusion area.

Where interacting clusters were present (forging "H") the individual irregular areas were determined and added together before a circle of equivalent total area was calculated (see Fig. 6).

In the case of irregular inclusion areas with non-uniformly distributed particles (forging "D") the whole specific inclusion area with low and high particle concentration was determined for the approximation of the equivalent circle (see Fig. 5).

The fracture mechanics evaluation was performed by comparison of these ΔK-values with the threshold stress intensity amplitude, ΔK_o, determined at the same R-value on compact tension specimens taken in the same orientation from adjoining defect-free regions of the same forgings. The ΔK_o-values were carefully determined by small incremental step decreases of the loading amplitude while monitoring the crack with the potential drop technique. On the basis of fracture mechanics, i.e., if the inclusion areas behave as sharp cracks, fatigue cracking would be expected at all flaws for which ΔK lies above ΔK_o.

RESULTS AND DISCUSSION

Figure 3 shows the results of the evaluation of the fracture surfaces. In all, 98 inclusions were examined on the fracture surfaces of the specimens taken from the 4 forgings. In each case the ΔK-values are plotted with open points indicating flaws at which no fatigue crack had nucleated and closed points showing those at which cracking was observed. Triangles mark

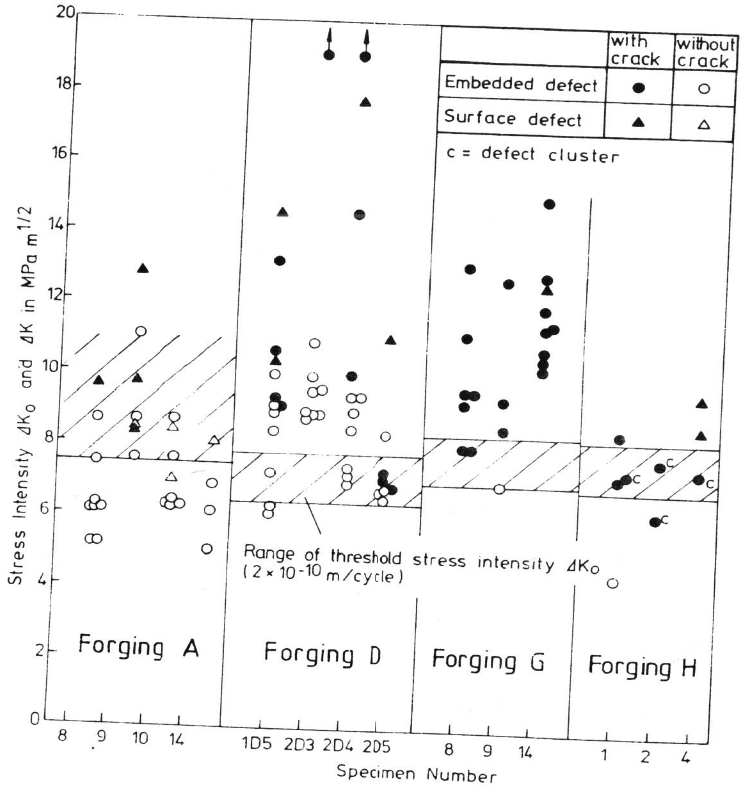

Fig. 3 Comparison of calculated ΔK values with measured threshold ΔK_o

surface defects and circles embedded ones. In addition a letter c adjacent to the symbol refers to a defect cluster where a single ΔK-value was calculated for a number of neighbouring flaws. The measured ΔK_o-values are shown on the same diagram and correspond to a propagation rate of 2×10^{-10} m/cycle. This corresponds to a distance of 5 mm at a magnification of 1000 X in the scanning microscope - the lower detection limit for the presence of a small fatigue crack. A scatter band has been added to the ΔK_o-values to account for the observed variability within the forgings tested.

For forging "A" a clear division is apparent. All of the elliptical flaws with Al_2O_3 inclusions showing ΔK-values below the ΔK_o-range have no fatigue cracks and the most with ΔK-values within the ΔK_o-range are devoid of fatigue cracks. This observation applies equally for surface and embedded flaws. A further clear-cut case is provided by forging "G" containing silicate inclusion areas. All inclusion areas are irregular individual flaws. In this case only one inclusion area could be found without a fatigue crack. Apparently the brittle fracture path is less likely to pass through uncracked silicate inclusion areas.

However discrepancies appear for the remaining two steels. Forging "D" clearly exhibits flaws possessing ΔK-values up to 50 % above ΔK_o but without evidence of fatigue cracking. This appears both for single flaws and groups of flaws. Closer examination of the inclusion areas and a comparison with those visible in forgings "A" and "G" indicate that the inclusion areas in "D" contain a non-uniform distribution of Al_2O_3 (rounded) and MnS (angular) particles so that it is inconceivable that the whole inclusion area used for the calculation of ΔK could immediately act as a crack. Figure 4 shows a typical SEM picture of a region within an inclusion

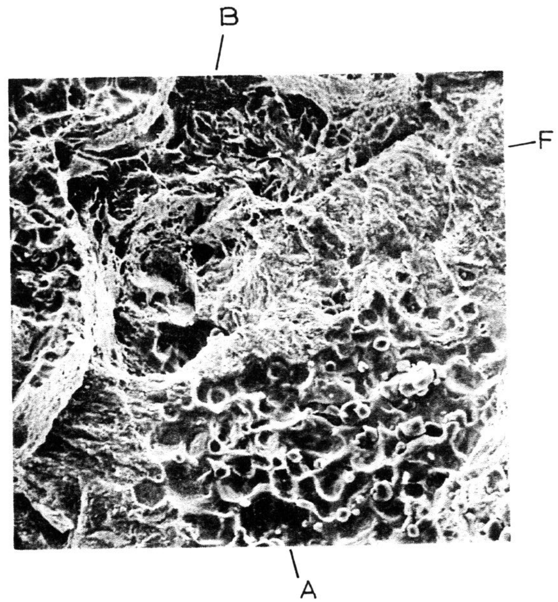

Fig. 4

Typical SEM picture in a region within an inclusion area after pulsating loading (forging D)

0.02 mm

of 0.35 mm² in size. Both fatigue crack (F) and brittle fracture (B) zones are visible within the inclusion area; ductile zones (A) can be seen around the particles. It would appear that the zones containing a high density of inclusion particles are cracked presumably during the first loading cycles. Fatigue cracks then propagate for a limited distance between the densely populated zones within the overall inclusion periphery. If the specimen is now broken open at low temperature the remaining zone will be brittle as shown in Fig. 4 and schematically in Fig. 5. This is the initial stage of the fatigue crack growth in such non-uniformly distributed particle areas. If, however, the fatigue loading is continued the crack will develop a

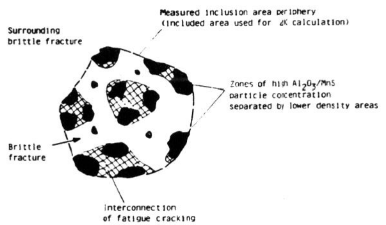

Fig. 5
Schematic diagram indicating how the process of fatigue cracking may occur within a defect in which the inclusions are non-uniformly distributed, e.g. in forging D (compare photograph in Fig. 4.)

circular form and propagate away from the inclusion area (Fig. 2b) This process is summarized in Fig. 5, i.e., when the inclusion area is only sparsely (non-uniformly) covered with particles the stress intensity amplitude must be raised well above ΔK_o before cracks which form at different points can grow together so that macroscopic fatigue cracking will be observed. Turning now to the results from forging "H", which contained solely fine irregular MnS inclusions, sometimes in association with pores, it is apparent that, although fatigue cracks are observed in all cases for ΔK above the ΔK_o-range and the absence of fatigue cracks is only observed below ΔK_o, some inclusions slightly below and at the bottom edge of the ΔK_o-band show considerable amounts of fatigue cracking. This is almost exclusively the case for defect clusters so that a discrepancy in the analysis may arise from the method used for the calculation. In such cases the individual inclusion areas lying in close proximity to one another have been added together and ΔK calculated for a circle of size equal to the summed areas (Fig. 6). For two adjacent circular cracks of equal size this leads to a 20 % higher ΔK-value than for the single crack. However, a recent photoelastic stress analysis of adjacent cracks (Phang 1983) has shown that as two equal-sized cracks are moved closer to one another the K-value at adjacent points on the crack circumference can be up to 1.5 times higher than for the single crack, so that the effective value of K at adjacent points on closely neighbouring inclusion areas could be up to 30 % higher than calculated in the present work and shown in Fig. 3, for example, for forging "H". An appropriate re-evaluation of the stress intensity values for inclusion clusters at all of which cracking was observed moves them, in line with other observations, into the upper range of or above ΔK_o.

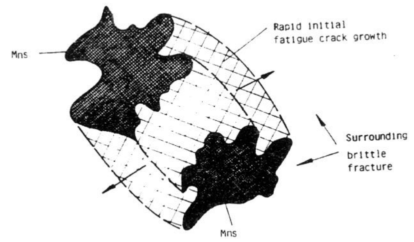

Fig. 6
Schematic diagram showing that for clusters of closely spaced inclusions local cracking occurs rapidly at adjacent points on their circumferences where the K-value is increased by their interaction (forging H)

Evidently the present summation procedure for the calculation of the total inclusion area for the determination of the ΔK-value of an irresolvable cluster underestimates the true value. In standards ASME XI and British Standard PD 6493 rules have been laid down stating that for the close approach of two cracks (separation less than average or smallest individual crack diameter) the encompassing crack should be used for the K-calculation. This provides values in rough agreement with the experimental photoelastic analysis indicating that it seems to be a realistic method.

We are now faced with the task of estimating the effective size of single defects and defect groups with a view to calculating their effective ΔK-values so that a prediction of their ability to propagate can be made by comparison with appropriate ΔK_o-determinations. In the case of separate compact flaws (forgings "A" and "G") the US inspection reveals a defect area which is used to calculate ΔK, which in turn, through comparison with ΔK_o, provides a reliable prediction of the flaws's ability to nucleate a fatigue crack. Where the flaws are present either separately or as clusters and the inclusion areas are only sparsely (non-uniformly) populated with particles (forging "D") the calculation of the ΔK-values from the inclusion area may lead to conservative results, i.e, no growth occurs even for ΔK-values slightly in excess of ΔK_o. However, in the case of clusters of flaws which are densely populated with particles (forging "H") ΔK-values determined from the total defect area, which is related to the resultant US signal, can lead to non-conservative results, i.e. cracks propagate at ΔK levels somewhat below ΔK_o. In this case a safe prediction can only be obtained if rules such as those laid down in British and ASME standards are employed.

CONCLUSIONS

The results of the present work indicate that the evaluation of the fatigue cracking behaviour of steel-making inclusions can be performed satisfactorily using linear elastic fracture mechanics principles provided that the inclusions are present in the form of regions containing densely packed particles. On the other hand, the effect of single inclusions not consisting of densely packed regions may be overestimated. Methods for the correct evaluation of closely spaced clusters must be further developed to permit a satisfactory evaluation of their effective stress intensity values.

ACKNOWLEDGEMENTS

The authors would like to express their thanks to the Forschungsvereinigung für Verbrennungskraftmaschinen for the provision of finances with which a major part of the work was performed, to the Industrieanlagen Betriebsgesellschaft mbH (IABG) at which the tests were carried out and especially to the members of the advisory group which provided invaluable help during the course of the work.

REFERENCES

Friedl, K. H., Scarlin, R. B. and Zelizko, V., Advances in Fracture Research, ICF5, 29 March - 3 April 1981, Cannes, France, Vol. 2, p. 923.

Harkegard, G., Eng. Fract. Mech., 6, Dec. 1974, 795.

Elsender, A., Gallimore, R. and Poynton, W.A., Fracture 1977, ICF4, June 19 - 24, Waterloo, Canada, Vol. 2, p. 953.

Melville, P. H., Conference on Fracture Mechanics in Engineering Practice, Sheffield, Sept. 1976, CEGB Report LM/MATS/098

Phang, Y. and Ruiz, C., Conference on Application of Fracture Mechanics to Materials and Structures, June 20 - 24, 1983, Freiburg, Germany, Proceedings in press.